

Self-balancing Control Strategy for a Battery Based H-Bridge Multilevel Inverter.

Juan Guavita, Rafael Diez, Diego Patiño, Fredy Ruiz

Dept. of Electronics Engineering

Pontificia Universidad Javeriana

Bogotá, Colombia

Email: {jguavita, rdiez, patino-d, ruizf}@javeriana.edu.co

Gabriel Perilla

Dept. of Electronics Engineering

Universidad Nacional de Colombia

Bogotá, Colombia

Email: gperillag@unal.edu.co

Abstract—this paper presents a novel control strategy for isolated multilevel inverters. This converter has been chosen due to the autonomy of each full bridge. Other advantage is the feasibility of handling the power by cell when there are changes in the batteries state of charge (SOC). In order to take advantage of these benefits, a control strategy has been developed. The main goal of the proposed solution is to change the power produced by each inverter in function of SOC, guaranteeing a proper regulation of the overall power, without affecting the parameters of quality of the output voltage like harmonic distortion and amplitude. The designed solution was tested by power sources variations, finding the control strategy appropriate to accomplish the objective, to modify the power produced by each full bridge in function of SOC without changing overall power of the system and keeping the output voltage constant.

Index Terms— Modular multilevel inverters, pulse width modulation converters, state-of-charge (SOC) balancing, DC-AC power converters.

I. INTRODUCTION

The increasing consumption of energy, the negative environmental impact produced by the fossil fuel based generation due to the emission of greenhouse effect gases had created an upraise interest in renewable energy technologies [1,2]. One of those solutions is based on photovoltaic technology, where solar energy is transformed in electric energy [3]. This technology has been developed for the last years due to the increasing demand of this kind of energy. The requirement of this technology has grown between 20% to 25% per annum over the past 20 years due to the decreasing costs and prices [3]. This phenomenon is caused by manufacturing improvements and economies of scale [4]. One of the devices which has shown significant manufacturing improvements is the PV inverter [5]. Usually in PV standalone systems, the available generated power and the required power by the load are not equal. For this reason, the use of batteries is required to store the excess of energy [6] [7]. Therefore, several topologies of inverters have been developed in order to improve the quality of the energy. Nowadays, the multilevel inverters (MLI) have become more attractive for researchers and manufacturers due to their improvements in the output waveforms, smaller filter size, lower EMI and lower total harmonics distortion (THD)

[6,7]. There are three common topologies for multilevel inverters like capacitor clamped [8,9], diode clamped [10,11] and cascade full bridge inverter [12,13]. Among the topologies of multilevel inverters, the cascade full bridge inverter is a promising alternative due to its modular design. It allows achieving a low harmonic output voltage without leaving behind its redundancy due to its separate DC-sourced full-bridge cells [14,15]. These characteristics allow to think in a solution where the power delivered by each full bridge inverter can be handled in function of SOC, without disrupting the requested output voltage [16].

In this field, other researchers have developed control strategies where is possible to bypass a faulty inverter without upsetting the power delivered to the load. It is possible due to the feasibility of the other inverters to produce the extra power in correlational ratio [17]. These kinds of solutions are required due to the lack of robustness in the isolated PV systems where a half bridge inverter with a unique power source and limited harmonic reduction is commonly used [18]. Those systems exhibit problems with the produced power, because the inverter depends on the state of charge of one group of batteries. Whether the state of charge drops out, the inverter with only one source of power cannot deliver the requested energy [19]. Some solutions have been proposed to solve this problem. They include topologies and control strategies with bidirectional DC/DC converters, whose function is to manage the state of charge of the batteries [20, 21]. In this kind of standalone systems, the control strategy for the inverter is not employed to solve the issues with the SOC.

Therefore, this paper proposes a battery based full bridge multilevel inverter to be used in standalone systems. This topology allows to avoid the dependence of the system to just one string of batteries thanks to its modularity. In order to take advantage of the features of the MLI, this paper is devoted to present a self-balancing control strategy for a battery based full bridge multilevel inverter. The main goal of the strategy is to manipulate the delivered power of each cell in function of SOC. The paper is organized as follows: In section II, a brief description of the main characteristics of MLI is presented and the control principle is explained in section III. The results are exposed in section IV. The conclusions and future works are presented in the last section.

II. THE SYSTEM TOPOLOGY

The cascade multilevel inverter topology consists of n full bridges connected in series. Each cell is fed by a string of Batteries. Fig.1. Shows the topology of the inverter. Each cell uses a DC-link voltage to generate a modulated voltage at the output terminal. The total output voltage V_{diff} is obtained by the sum of the voltage generated by each full bridge. Each cell can produce a total of three levels of voltage: $+v_{dc}$, $-v_{dc}$ and 0. Therefore, the number of voltage levels in open loop is given by:

$$\#_{levels} = 2N_{inv} + 1 \quad (1)$$

In this case, The MLI has five inverters; the total amount of levels is eleven. The output filter is used to take the commutation noise away. This filter needs to guarantee its frequency of operation at least two decades less than commutation frequency. In this case, the commutation frequency of each cell is 50 KHz. Therefore, the output commutation frequency is by 500 KHz. For this case the filter frequency operation is calculated in 5 KHz. Other parameter of operation is that the impedance should be less than twice the value of the maximum charge. The input filter of each full bridge has the goal of protect the sources of the AC component of the current.

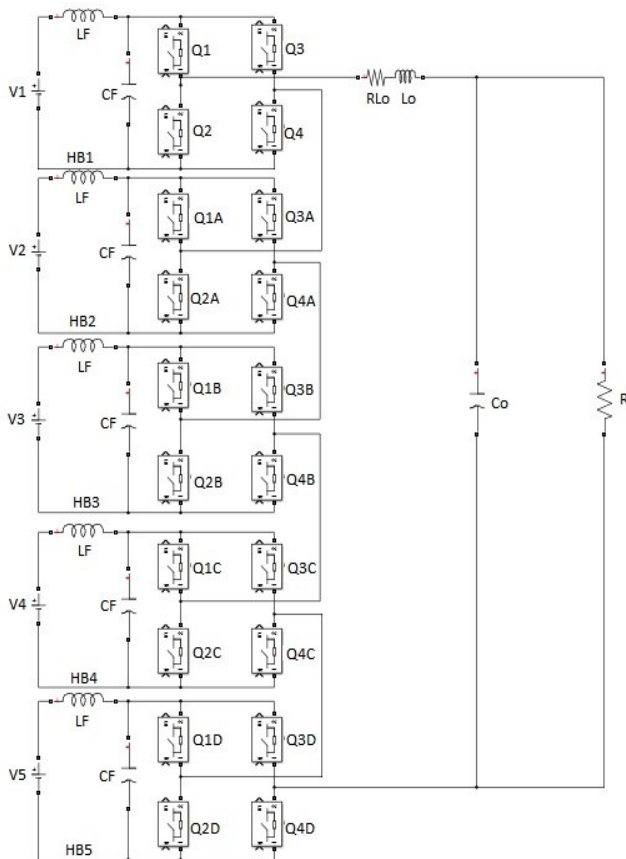


Fig. 1. Single-phase Cascade H-Bridge Multilevel Inverter.

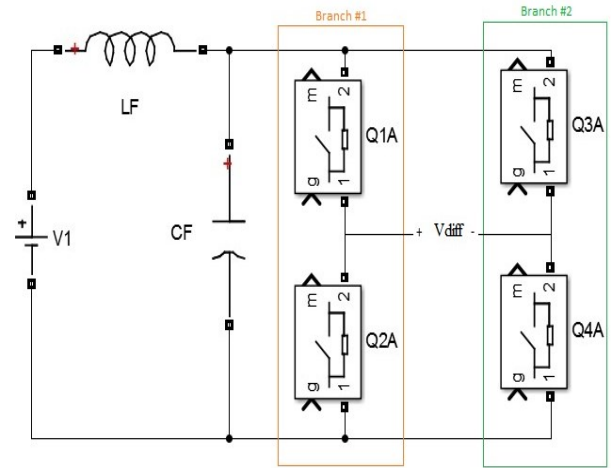


Fig. 2. H-bridge Topology.

In order to produce the voltage in each H-bridge, each one needs two modulating signals and one carrier signal to generate the modulated signals. Fig. 2 shows the topology of one H-bridge. Each one is composed by two branches. Each branch has two mosfet and changes its voltage between 0V and 48V for this case. Each cell needs two modulating signals and one carrier signal to generate the modulated signals. The Fig. 3 shows the signals of the cell of power. Where V_{m+} and V_{m-} are the couple of modulating signals and the triangle signal V_t is the carrier signal. The modulating signals have a frequency of 60 Hz with a phase of 180° between them. The same modulating signals are employed by all the cells. In contrast, the frequency value of the carrier signal is the commutation frequency. The carrier signals of each cell are dephased by 72° , in order to properly add the output voltages. This information is important to understand the control strategy that will be explain later.

Likewise, there is a need to analyze the behavior of the system when there are changes in the batteries that feeds each cell. The Fig. 4 shows the output voltage of the MLI in open loop when there is a disrupt in the batteries that feeds each H-bridges.

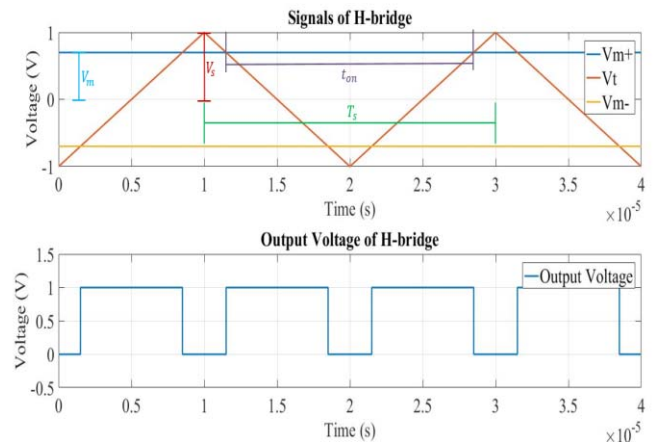


Fig. 3. Signals of the Inverter.

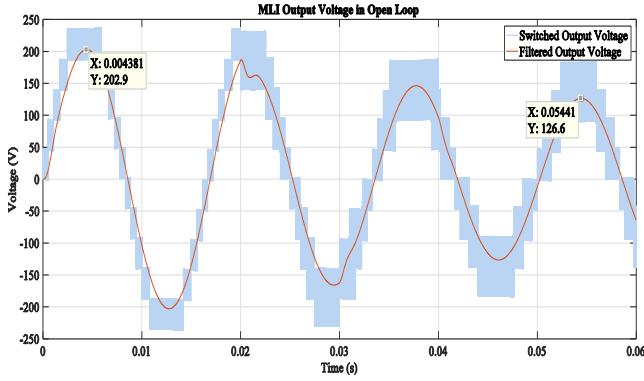


Fig. 4. System and Model Response with deviation in the batteries.

Where V_1, V_2, V_3, V_4, V_5 are the batteries string of each cell of power. In this case V_1 has a voltage reduction between 48V to 42V. likewise, V_2 and V_4 have a change between 48V to 45V. In this case the output voltage has an amplitude of 200 V. when the change in the DC sources occurs, the output voltage presents a variation of 37% in its amplitude. This result shows the requirement of a control strategy a control strategy in order to keep the output voltage constant regardless the DC voltage of each H-bridge battery.

III. CONTROL STRATEGY

The control strategy should accomplish two objectives: The first objective is to manage the delivered voltage of each cell in order to self-balance the SOC of the H-bridges batteries. The second one is to keep the output voltage stable.

The main idea of the first part of the control strategy is to manage the power of each cell according to the state of charge of the batteries. Let t_{on1} be the turn on time of the mosfet Q1N (showed in Fig.3), T_s the switched frequency, V_s the amplitude of the carrier signal, V_1 the voltage of the batteries string and V_{m1} , the amplitude of the modulating signal. It is possible to establish a relation between variables of interest for one cell in equation (2) and (3):

$$\frac{t_{on1}}{T_s} = \frac{V_{m1} + V_s}{2V_s} \quad (2)$$

$$V_{dif} = \frac{V_{m1}}{V_s} V_1 \quad (3)$$

The equation (3) shows the relation between the output voltage of the cell, the amplitude of the couple of the modulating signals, the amplitude of the carrier signal and the voltage of the batteries. Then the expression (4) is developed using (2) and (3) where I_0 is the amplitude of the output current and I_1 is the value of the current of one cell:

$$I_1 = \frac{V_{m1}}{V_s} * I_0 \quad (4)$$

Equation (4) shows the relation between the current of one cell and the amplitude of the output current of the H-bridge. This equation is multiplied by a factor composed by the ratio between the amplitude of modulated and carrier signal. The same analysis is made in the other cells. This allows to gather an expression where $V_{m1}, V_{m2}, V_{m3}, V_{m4}, V_{m5}$ is the amplitude of the modulated signal and the batteries voltage of each cell V_1, V_2, V_3, V_4, V_5 is related:

$$\frac{V_{m1}}{V_1} = \frac{V_{m2}}{V_2} = \frac{V_{m3}}{V_3} = \frac{V_{m4}}{V_4} = \frac{V_{m5}}{V_5} = K \quad (5)$$

The last relation is possible due to the fact that modulating signals of each H-bridge are equals. Let equations (2) to (5), V_1 the voltage of the batteries, V_1, V_2, V_3, V_4, V_5 the other voltages of the batteries of each cell and the sinusoidal function which is the control signal generated due to the error between the output voltage and the reference. Knowing that the output voltage of the multilevel inverter is the sum of the output voltage of each inverter, the equation (10) shows the relation between the amplitude of the modulating signal used to manage the commutation of the H-bridge.

$$V_{m1} = \frac{V_s * V_p \text{sen}(wt) * V_1}{V_1^2 + V_2^2 + V_3^2 + V_4^2 + V_5^2} \quad (6)$$

This equation uses the voltage of all the independent sources of each cell to handle the amplitude of the modulated signal. This result is important due to the option to modify the amplitude of the modulating signal reciprocal to the value of the level voltage in the source of the cell. In this control strategy, the signal is the same for all the H-bridges. Therefore, whether one of the modulated signal changes because the feeding voltage changes, the other modulated signals will modify its amplitude in order to keep the total amount of power requested by the load. The equation (11) shows the relation between the delivered current of each cell and the batteries string that feeds the cell where P_o is the output power of the system:

$$I_1 = \frac{P_o}{(V_1^2 + V_2^2 + V_3^2 + V_4^2 + V_5^2)} * V_1 \quad (7)$$

So the information of each DC source is available for each modulated signal. It allows to modify the signal in function of the battery voltages as well as the other batteries that fed the other cells. The first part of the control strategy shows how to manipulate the power of each H-bridge in function of the batteries state of charge. To accomplish the objective of keeping the output power constant, a PI controller is implemented for this simulation. For its design, an average model is developed. This model allows to analyze the behavior of the system in order to design the correct controller. The Fig.5 shows a block diagram of the system, in order to see the elation of the PI controller and the self-balancing part of the control. The controller generates

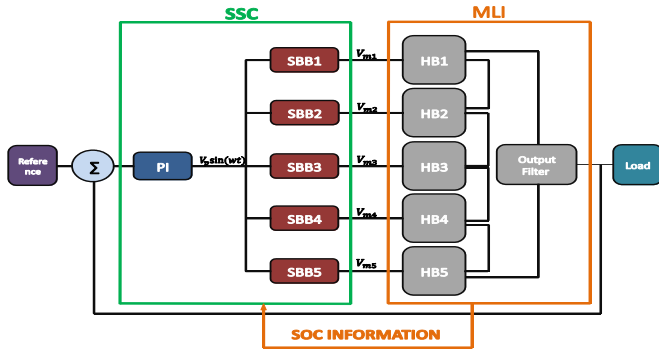


Fig. 5. Block Diagram of the control strategy.

the control signal as a result of the error between the output voltage and the reference of the system. The control signal is modified in amplitude by the SBB block in order to generate the modulating signal of each H-bridge using (6) to modify its amplitude according to SOC. The connections of each SBB block are shown in Fig. 6. This figure shows the required values to make the balance of the charge. Each block needs the information about the SOC of all the batteries presented in the system, the control signal of the PI controller and the amplitude of the carrier signal. This information allows to generate the modulating signal.

IV. RESULTS.

To estimate the performance of the control strategy, it is compare with a classic PI control strategy. Both strategies are submitted to the same conditions. The MLI has a linear load in parallel with a rectifier. The output current is 5.30 A. The batteries have the same voltage at the beginning of the test. To simulate the batteries, each cell is fed by a DC controlled voltage source to simulate the slow changes presented in a real battery. The Fig. 7 shows the variations of the voltage of each DC source. In this case, the DC sources V1 has a variation in its voltage between 48 V and 42 V. Likewise V3 have variations in between 48 V and 45 V. The Fig.7 shows the variations of the voltage of each DC source. In this case, the DC sources V1 has a variation in its voltage between 48 V and 42 V. Likewise V3 have variations in between 48 V and 45 V. Fig. 7 shows the results of the simulation of the system with the propose strategy. The slow tendency of discharge is used here because these sources represent a string of batteries.

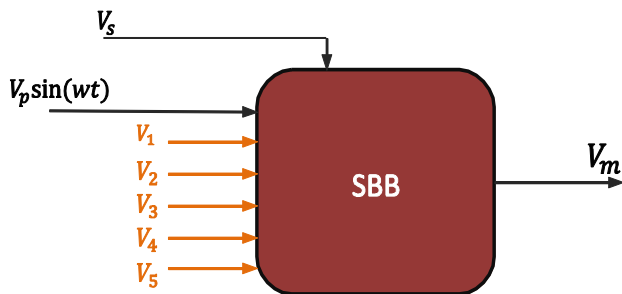


Fig. 6. Signals of Self-Balancing Block. (SBB).

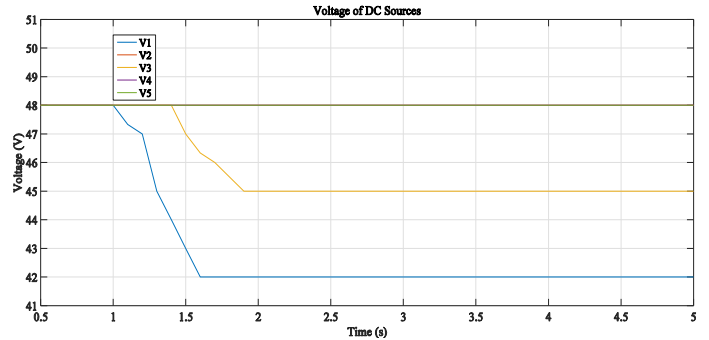


Fig. 7. Disrupt in the voltage of the batteries.

In standalone systems, the batteries are used to feed each H-bridge where its discharge is slow. Therefore, there is a need to simulate an approximate behavior of the batteries in order to evaluate the performance of the batteries. The Fig.8.a shows the behavior of the delivered current by each DC source when the propose solution is set on the system (II+SSB). The self-balancing control reduces the amount of current produced by the DC source when the voltage of the battery decreases. Besides, the solution increases the current production of the other batteries in order to keep the overall power. The Tab. 1 shows the values of current and power of each DC source during the test with self-balancing solution, compose by the controller PI and the SBB blocks. These values shown the initial and final values of the currents of each battery. In this case, V1 y V3 show changes in its voltage. The initial value of the currents is 3.8 A. This value is the same for all the batteries due to the initial voltage is the same for all the sources. The final values of the currents changes thanks to the changes shown in the Fig. 7. IB1 presents a decrease in its value due to fall in V1. The change in V1 is the first change to be correct in the system by the control strategy. Afterwards there is a change in V3. In this case, the change is less than the change in V1. The others sources V2, V4, V5 do not present changes in its voltages; it let this sources to contribute with the maximum amount

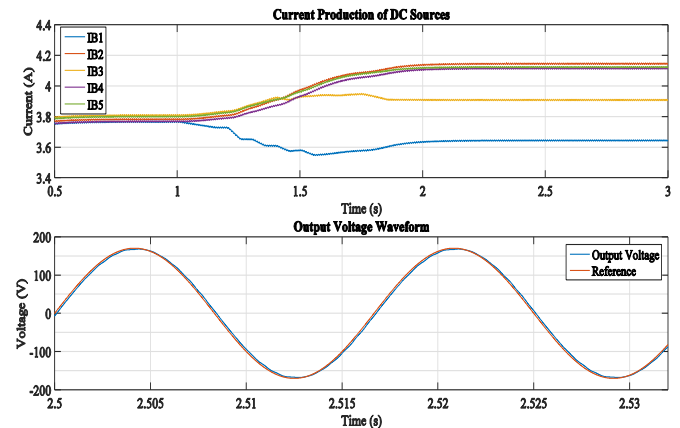


Fig. 8a). Current Produced by each DC source with PI+SBB. 8b). Output voltage response with Self-Balancing solution.

Current	IB1	IB2	IB3	IB4	IB5
I. Val	3.80 A	3.80 A	3.80 A	3.80 A	3.80 A
F. Val	3.64 A	4.10 A	3.90 A	4.10 A	4.10 A
Power	FB1	FB2	FB3	FB4	FB5
Initial: 912 W	182.4 W	182.4 W	182.4 W	182.4 W	182.4 W
Final: 918 W	152.8 W	196.8 W	175.5 W	196.8 W	196.8 W

Tab. 1. Current and Power Variations of the Batteries with PI+SBB controller.

Of power. The changes in the power produce by each H- Bridge are shown in the same table. The cell of power one and three, called FB1 and FB3, shows the expected decrease of power. FB1 presents a decrement of 16.2%. In the same way, FB3 shows a change in its produced power of 3.71%. Otherwise, FB2, FB4 and FB5 that represent the other H-bridge, show an equivalent increment of 7.8 % in the produced power. Moreover, there is a require to analyses the total amount of produced power by the whole cells of power. The control strategy allows to change the power produced by each cell without change the overall amount delivered by the MLI. Now, the results of the test with the system with the classic PI controller are shown below. Fig. 9a. shows the current delivered by each source.

In this case, the classic PI controller tends to correct the change in the DC voltage like the propose solution. In this case, the control action increases the current of each DC source proportionally regardless the voltage of each source. Tab. 2 shows the values of the variables with a classic PI controller. When the changes in the sources V1 and V3 occurs, the controller increases the currents of all the sources. In this opportunity, all the sources have an increase in its current production of 4.45%. It occurs when V1 and V3 should produce less current due to the decrease in its voltage. This control action reduces the duty cycle of the batteries.

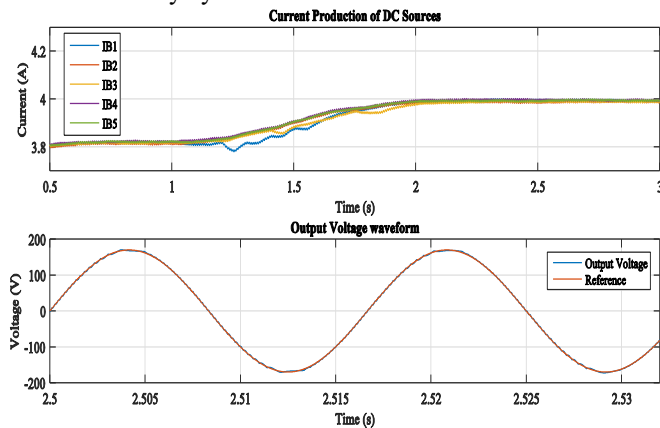


Fig. 9a). Current Production by each DC source with classic PI controller. 9b) Output voltage system without Self-Balancing solution.

Current	IB1	IB2	IB3	IB4	IB5
I. Val	3.80 A	3.80 A	3.80 A	3.80 A	3.80 A
F. Val	3.99A	3.99 A	3.99 A	3.99 A	3.99 A
Power	FB1	FB2	FB3	FB4	FB5
Initial: 912 W	182.4 W	182.4 W	182.4 W	182.4 W	182.4 W
Final: 921 W	167.5 W	191.5 W	179.5 W	191.5 W	191.5 W

Tab. 2. Current and Power Variations of the Batteries with PI controller.

Likewise, table 1, it shows the changes in the power produce by each H- Bridge with the classic PI controller. Now, FB1 and FB3 shows a decrease of power. FB1 presents a decrement of 9.13%. In the same way, FB3 shows a change in its produced power of 2.07%. Otherwise, FB2, FB4 and FB5 that represent the other H-bridge, show an equivalent increment of 4.47 % in the produced power. The control strategy allows to change the power produced by each cell without change the overall amount delivered by the MLI like the propose solution. In the test, V1 reach the minimum voltage allowed in the batteries in a standalone system. In this case, the voltage source gives the minimum amount of power allowed in the system. likewise, V3 is reduced in a less proportion.

Those variations are made to show the behavior of FB3. In this stage, FB3 has to deliver some of the power that FB1 cannot deliver due to its condition regardless the change presented in its voltage. Afterwards, the performance of the controllers to keep the output voltage constant is showed. The Tab.3 shows the characteristics of the output voltage. The values of the table exhibit a similar behavior in both strategies regardless the modification on the amplitude made by the SBB block in the propose solution.

The output voltage has a steady state error less than 1%. The total harmonic distortion in both cases are less than 5%. This values stay constant in the propose solution regardless the presence of the SBB block. Finally, The Fig. 10 shows the output voltage of the MLI with its component of commutation correlate with the output signal of the output filter. This image shows the changes in the commutate voltage of the MLI where there are reciprocal changes between sources voltages and currents. The figure shows additional levels to the eleven mentioned by MLI with five H-bridges.

Strategy.	Amplitude	SSE.	%THD
KI+SBB	169.13 V	0.87 V	4.79
KI	169.14	0.86 V	4.74

Tab. 3. Characteristics of the Output voltage.

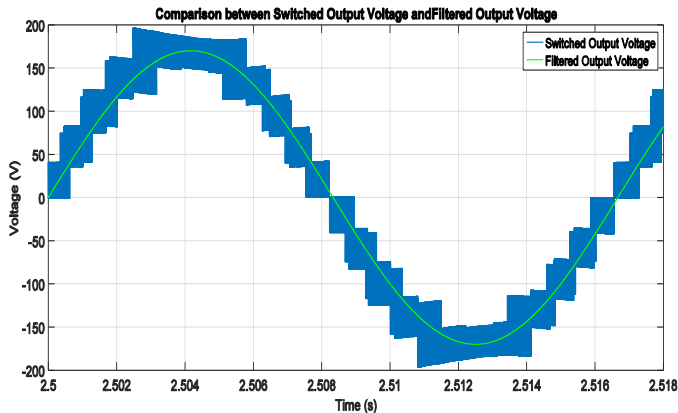


Fig. 10. Commutate output voltage levels and Filtered Output Voltage.

V. CONCLUSIONS AND FUTURE WORK.

A novel control strategy for self-balancing power had been presented for battery based multilevel inverters. This solution allowed to manipulate the power of each cell in function of the state of charge of the batteries (SOC). The low complexity of the solution allowed to think in a fast-online installation. Such as was exposed, the strategy presented two main parts: the first part was a high level control which function was to manipulate the power of each cell when there were changes in SOC. The second one was to keep the output voltage constant when there were changes in the produced power of each cell. This part was accomplished with a PI controller. The comparison between the classic PI controller with the self-balancing control strategy showed similar values of performance to keep the output voltage in acceptable conditions. The difference between both strategies was in the power produced by each H-bridge. In the self-balancing strategy control, the power of each cell was manipulated to reduce the power requested to the less charged batteries. Whereas, the classic PI controller made the same changes in the power of each DC source regardless the DC voltage of the sources.

The next step in the project will be to set the strategy up in a real MLI, to evaluate the behavior of the strategy in a real inverter.

ACKNOWLEDGMENT.

This work was supported by Fondo de Ciencia y Tecnología e Innovación del Sistema General de Regalías (SGR), Gobernación de Cundinamarca (Colombia), convenio especial de cooperación No. SCTeI 016 de 2015.

VI. REFERENCES

[1] H. Farhangi, «The path of the smart grid,» *Power and Energy Magazine*, pp. 18-28, 2010.
 [2] G. A. a. L. T. ackerman, «Distributed generation: a definition,» *Electric Power System Research*, pp. 195-204, 2001.

[3] N. A. R. S. M. Jeyraj Selvaraj, «Multilevel Inverter For Grid-Connected PV System,» *IEEE TRANSACTIONS ON INDUSTRIAL ELECTRONICS*, 2009.
 [4] L. G. F. J. T. B. E. G. R. C. P. M. A. M. P. J. I. L. a. N.-A. J. M. Carrasco, «Power electronic systems for the grid integration of renewable energy sources: A survey,» *IEEE Transactions on industrial electronics.*, pp. 1002-1016, 2006.
 [5] W. B. L. a. C. V. N. V. G. Agelidis. D. M. Baker, «A Multilevel PWM inverter topologu for photovoltaic applications,» *IEEE ISIE*, pp. 589-594, 1997.
 [6] J. R. a. J. R. S. Kouro, «Reduced switching-frequency modulation algorithm for high-power multilevel inverters,» *IEEE transactions in electronic industries*, pp. 2894-2901, 2007.
 [7] S. G. M. M. R. S. a. G. S. G. Carrara, «A new multilevel PWM method: A theoretical analysis,» *IEEE Transactions in Power electronics*, pp. 497-505, 1992.
 [8] T. M. a. H. Foch, «Multi-level choppers for high voltage applications,» *European Power Electronics*, pp. 45-50, 1992.
 [9] B.-R. L. a. C.-H. Huang, «Implementation of a three-phase capacitor clamped,» *IEEE Transactions in industrial electronic*, pp. 1621-1630, 2006.
 [10] A. Nabae and H. Akagi, «A new neutral-point clamped PWM inverter,» *IEEE Transactions in industrial applications*, pp. 518-523, 1981.
 [11] S. B.-M. J. B. J. G. D. G. a. J. B. S. Alepuz, «Interfacing renewable energy sources to the utility grid using a three-level inverter,» *IEEE Transactions in Industrial Electronics*, pp. 1504-1511, 2006.
 [12] M. M. a. S. T. M. Marchesoni, «A non conventional power converter for plasma stabilization,» *IEEE Power Electronics*, pp. 122-129, 1988.
 [13] K. C. a. M. W. X. Kou, «Overdistention operation of cascaded multilevel inverters,» *IEEE Transactions in Industrial Applications*, pp. 817-824, 2006.
 [14] J.-S. L. a. F. Z. P. J. Rodriguez, «Multicarrier PWM strategies for multilevel inverters,» *IEEE Transactions in industrial electronics*, p. 738, 2002.
 [15] V. G. A. a. M. S. D. M. Calais, «A cascaded inverter for transformerless single phase grid-connected photovoltaic systems,» *Proc. 31st Annu. IEEE PESC*, pp. 1173-1178, 2001.
 [16] A. D. M. L. a. V. M. C. Cecati, «A passivity based multilevel active rectifier with adaptive compensation for traction applications,» *IEEE Transactions in Industrial Applications*, pp. 1404-1413, 2003.
 [17] S. M. I. K. G. S. M. I. Mariusz Malinowski, «A Survey on Cascaded Multilevel Inverters,» *IEEE TRANSACTIONS ON INDUSTRIAL ELECTRONICS*, 2010.
 [18] J. G. D. U. S. Andreas Joossen, «Operation conditions of batteries in PV applications,» *Solar Energy*, 2003.
 [19] M. A. M. N. Achaiboua, «Modeling of lead acid batteries in PV systems,» *SciVerse ScienceDirect*, pp. 538-544, 2012.
 [20] D. M. J. J. Hisham Mahmood, «Control Strategy for a Standalone PV Battery,» *IEEE*, pp. 3412-3418, 2010.
 [21] A. Q. H. X. Y. Yen-Mo Chen, «A High Step-Up Three-Port DC-DC Converter for,» *IEEE TRANSACTIONS ON POWER ELECTRONICS*, vol. 28, n° 11, pp. 5049-5062, 2013.

